

Galactic structure studies from BATC survey

Cuihua Du^{1,2}, * Jun Ma², Zhenyu Wu² and Xu Zhou²

¹College of Physical Sciences, Graduate university of the Chinese Academy of Sciences, Beijing 100049, P. R. China

²National Astronomical Observatories, Chinese Academy of Sciences, Beijing 100012, P. R. China

Received

ABSTRACT

We present an analysis of the photometric parallaxes of stars in 21 BATC fields carried out with the National Astronomical Observatories (NAOC) 60/90 cm Schmidt Telescope in 15 intermediate-band filters from 3000 to 10000 Å. In this study, we have adopted a three-component (thin disk, thick disk and halo) model to analyze star counts information. By calculating the stellar space density as a function of distance from the Galactic plane, we determine that the range of scale height for the thin disk varies from 220 to 320 pc. Although 220 pc seems an extreme value, it is close to the lower limit in the literature. The range of scale height for the thick disk is from 600 to 1100 pc, and the corresponding space number density normalization is 7.0-1.0% of the thin disk. We find that the scale height of the disk may be variable with observed direction, which cannot simply be attributed to statistical errors. Possibly the main reasons can be attributed to the disk (mainly the thick disk) is flared, with a scale height increasing with radius. The structure is consistent with merger origin for the thick disk formation. Adopting a de Vaucouleurs $r^{1/4}$ law halo, we also find that the axis ratio towards the Galactic center is somewhat flatter (~ 0.4), while the shape of the halo in the anticentre and antirotation direction is rounder with $c/a > 0.4$. Our results show that star counts in different lines of sight can be used directly to obtain a rough estimate of the shape of the stellar halo. Our solutions support the Galactic models with a flattened inner halo, possibly it is formed by a merger early in the Galaxy's history.

Key words: Galaxy: structure-Galaxy: fundamental parameters- Galaxy: stellar component-Galaxy: halo

1 INTRODUCTION

The detailed study of the Galactic structure enables us to address many important questions in astrophysics, for it is only in the Milky Way that we can make detailed studies. But, since we observe our Galaxy from within it, we must use indirect tools such as star counts to probe its structure (Peiris 2000). The star counts method, which is predominantly used to study the general properties of the Galaxy, is a very effective way of constraining the structural parameters for the components of the Galaxy, while the density distribution of the Galaxy components are assumed similar to those of galaxies of the same Hubble type. In the standard model (Bahcall & Soneira 1980), the Galaxy is of Hubble type *Sbc*, consisting of an exponential disk and a spherical halo.

Over the past decades, considerable efforts have been undertaken to gain information about the structure and his-

tory of formation and evolution of our Galaxy. The Galactic structure models of varying degrees of complexity have been developed (Bahcall & Soneira 1980, 1984; Gilmore 1984; Robin & Crézé 1986; Reid & Majewski 1993; Méndez et al. 1996; Siegel et al. 2002). It is now apparent from several independent avenues of research that our Milky Way is much more complex system than we thought before.

Bahcall & Soneira (1980) established the first standard model, in which the Galaxy was simplified and parameterized by an exponential disk and a spheroid, the latter is characterized by a de Vaucouleurs profile. Later, future studies on this subject showed that the number of population components of the Galaxy increased from two to three. This new component (the thick disk) was introduced by Gilmore & Reid (1983), based on star counts towards the South Galactic pole. The new component is discussed by Gilmore & Wyse (1985) and Wyse & Gilmore (1986). The stellar population of the thick disk is distinct from that of the halo, and its existence is seen clearly in colour magnitude diagrams derived from star count survey (Gilmore et al. 1989, Chen

* E-mail: ducuihua@gucas.ac.cn

et al. 2001). Following the work of Gilmore & Reid (1983), three components model including the thin disk, thick disk and spheroid (halo) have become a common model for our Galaxy and has been used widely.

Up to now, the basic stellar components of the Milky Way are the thin disk, thick disk, stellar halo and central bulge, albeit that the inter-relationships and distinction amongst different components remain subject to some debate (Lemon et al. 2004). In the previous works, various models have been developed to describe the stellar populations of the Galaxy. In general, these models were based on the assumption of a suitable spatial density distribution, and on the observational luminosity function and colour-magnitude diagram for each stellar population (Bahcall & Soneira 1984; Reid & Majewski 1993) to fit the structural parameters by exploiting the measurements of colour and magnitudes. The canonical spatial density distribution is as follows: stellar distribution for thin disk and thick disk in cylindrical coordinates by radial and vertical exponentials law and for the halo by the de Vaucouleurs spheroid (Du et al. 2003; Karaali et al. 2004). Thus, the structure parameters can then be deduced by comparing model and star count data. Different parametrization of the Galactic components were tried by many authors (Bahcall & Soneira 1980; Gilmore 1984; Ojha et al. 1996; Chen et al. 2001; Karaali et al. 2003, 2004; Du et al. 2003; Kaempf et al. 2005). However, due to different and conflicting results from modelling of star counts, the spatial distribution of the Galactic components remain controversial. There is still some uncertainty about the exact characteristics of each Galactic component. But quantifying the properties of the stellar components of the Galaxy is of wide importance; they are closely related to stellar quantities such as distance, age, metallicity, and kinematics characteristics, which are necessary for understanding the formation and evolution of the Galaxy (Du et al. 2004b; Pohlen et al. 2004; Brook et al. 2005). These properties can be obtained by straightforward photometric and spectroscopic observation. At present, before the full exploitation of the huge spectral surveys (e.g. GAIA, SEGUE, LAMOST, etc) is possible, star counts based on all-sky photometric surveys is one of the few accessible methods for the study of the Galactic structure.

In this study, to better understand and study the Galactic structure, the Beijing-Arizona-Taiwan-Connecticut (BATC) multi-colour photometric survey further provides more new catalogues with the achievement of data observation and reduction. These catalogues are very useful in constraining the structure of the main components of the Galaxy. We will report our investigation of star count extending our research to include different direction data. The present discussion is a more complete and sophisticated investigation of a number of BATC selected fields. Section 2 describes the details of observations and data reduction. The object classification and the photometric parallaxes are found in Sect. 3. Sect. 4 deals with the space density distribution of stars in the direction used in the study. Finally, we summarize and discuss our main conclusions.

2 BATC OBSERVATIONS

2.1 BATC photometric system and data reduction

The BATC survey performs photometric observations with a large field multi-colour system. There are 15 intermediate-band filters in the BATC filter system, which covers an optical wavelength range from 3000 to 10000 Å (Fan et al. 1996; Zhou et al. 2001). The 60/90 cm f/3 Schmidt Telescope of National Astronomical Observatories (NAOC) was used, with a Ford Aerospace 2048×2048 CCD camera at its main focus. The field of view of the CCD is 58′ × 58′ with a pixel scale of 1′′.7.

The definition of magnitude for the BATC survey is in the AB system, which is a monochromatic flux system first introduced by Oke & Gunn (1983). The 4 Oke & Gunn (1983) standards which are used for flux calibration in the BATC survey are HD19445, HD84937, BD+262606 and BD+174708. The fluxes of the four stars have been recalibrated by Fukugita et al. (1996). Their magnitudes in the BATC system have slightly been corrected by cross-checking with data obtained on a number of photometric nights (Zhou et al. 2001).

Preliminary reductions of CCD frames, including bias subtraction and flat-fielding correction, were carried out with an automatic data reduction procedure called PIPELINE I, which has been developed for the BATC survey (Fan et al. 1996). The HST Guide star catalogue (GSC) (Jenkner et al. 1990) was then used for coordinate determination.

A PIPELINE II program based on the DAOPHOT II stellar photometric reduction package of Stetson (1987) was used to measure the magnitudes of point sources in the BATC CCD frames. The PIPELINE II reduction procedure was performed on each single CCD frame to get the point spread function (PSF) magnitude of each point source. The magnitudes were then calibrated to the BATC standard system (Zhou et al. 2003). The other sources of photometric error, including photo star and sky statistics, readout noise, random and systematic error from bias subtraction and flat fielding, and the PSF fitting, are all considered in PIPELINE II. The total estimated errors of each star are given in the final catalogue (Zhou et al. 2003). Stars that are detected in at least three filters are included in the final catalogue.

In Table 1, we list the parameters of the BATC filters. Col. (1) and col. (2) represent the ID of the BATC filters, col. (3) and col. (4) the central wavelengths and FWHM of the 15 BATC filters, respectively.

2.2 The directions

Most previous investigations have focused upon one or a few selected lines-of-sight directions generally either in small areas to great depth or over a large area to shallower depth (e.g., Gilmore & Reid 1983; Bahcall & Soneira 1984; Reid & Majewski 1993; Reid et al. 1996). The deep fields are small with corresponding poor statistical weight, and the large fields are limited with shallower depth which may not be able to probe the Galaxy at large distance (Karaali et al. 2004). However, investigation into Galactic structure such as quantifying the properties of the stellar components and substructure of the Galaxy obviously benefit from large scale

Table 1. Parameters of the BATC filters

No.	Filter	Wavelength (Å)	FWHM (Å)
1	<i>a</i>	3371.5	359
2	<i>b</i>	3906.9	291
3	<i>c</i>	4193.5	309
4	<i>d</i>	4540.0	332
5	<i>e</i>	4925.0	374
6	<i>f</i>	5266.8	344
7	<i>g</i>	5789.9	289
8	<i>h</i>	6073.9	308
9	<i>i</i>	6655.9	491
10	<i>j</i>	7057.4	238
11	<i>k</i>	7546.3	192
12	<i>m</i>	8023.2	255
13	<i>n</i>	8484.3	167
14	<i>o</i>	9182.2	247
15	<i>p</i>	9738.5	275

surveys. In addition, evaluation of star counts in a single direction can lead to degenerate density-law solution. For instance, increasing the normalization of the Galactic spheroid and decreasing its axis ratio represent a degeneracy. This means that in most directions, one cannot distinguish between models with a flattened spheroid plus a low normalization ratio of spheroid stars to disk stars, and those with a high axis ratio plus a high normalization (Peiris 2000). Up to now, only a few programs survey the Galaxy in multiple directions such as the Basle Halo Program (Buser et al. 1999), the Besancon program (Robin et al. 1996, 2003), the APS-POSS program (Larsen & Humphreys 1996), and the SDSS (Chen et al. 2001)

In this paper, the BATC photometry survey presented 21 selected fields in the multiple directions. Each field of view is $\sim 1 \text{ deg}^2$. Table 2 lists the locations of the observed fields toward the Galactic center and their general characteristics. In Table 2, Column 1 represents the BATC field name; Columns 2 and 3 represent the right ascension and declination, respectively; Column 4 represents the epoch; Columns 5 and 6 represent the Galactic longitude and latitude; and the last two columns represent the mean reddening and limit magnitude, respectively. The mean reddening $[E(B - V)]$ were determined using the maps of Burstein & Heiles (1982). It is obvious that the effects of interstellar extinction is small for most fields. As shown in the Table 2, the most photometric depth of our data is 21.0 mag. in *i* band.

The fields used in this paper are towards the Galactic center, the anticentre, the antirotation direction at median and high latitudes, $|b| > 35^\circ$. The fields towards the anticentre and antirotation directions constrain the structure parameters towards the outer part of the Galaxy, and the fields towards the Galactic center constrain the inner part of the Galaxy. Since star counts at high Galactic latitudes are not strongly related to the radial distribution, they are well suited to study the vertical distribution of the Galaxy.

3 OBJECT CLASSIFICATION AND PHOTOMETRIC PARALLAXES

Since there are 15 intermediate-band filters with an optical wavelength range from 3000 to 10000 Å in the BATC multi-colour system. Every object observed in all BATC fields could be classified according to their SED information constructed from the 15-colour photometric catalogue. Here, because our fields in this work have also been observed by the Sloan Digital Space Survey (SDSS-DR4) and each object type (stars-galaxies-QSO) has been given. Thus, we can obtain a relative reliable star catalogue.

The observed colour of each star are compared with a colour library of known stars with the same photometric system. The input library for stellar spectra is the Pickles (1998) catalogue. This library consists of 131 flux-calibrated spectra, including all normal spectral types and luminosity classes at solar abundance, and metal-poor and metal-rich F–G dwarfs and G–K giant components. Our sample may contain stars spread over a range of different metallicities. In Fig. 1, the two-colour diagram (*d*–*i*) versus (*i*–*m*) is shown for our sample. The panel (a) represents the northern sample (north of the Galactic plane), and the panel (b) represents the southern sample (south of the Galactic plane). Although the 15 filters are used in the object classification, the two-colour diagram based only on the *d*, *i*, *m* filters as an example shows that the scatter still exists in our sample. Most of stars lie in the mean main sequence track, and for those objects beyond the track, the scatter can be mainly due to the metallicity effect and a few non-main sequence stars contamination.

For those stars, the probability of belonging to a certain star class is computed by the SED fitting method. The standard χ^2 minimization, i.e., computing and minimizing the deviations between photometric SED of a star and the template SEDs obtained with the same photometric system, is used in the fitting process. The minimum χ^2_{min} indicates the best fit to the observed SED by the set of template spectra:

$$\chi^2 = \sum_{l=1}^{N_{fit}=15} \left[\frac{F_{obs,l} - F_{temp,l} - b}{\sigma_l} \right]^2, \quad (1)$$

where $F_{obs,l}$, $F_{temp,l}$ and σ_l are the observed fluxes, template fluxes and their observed uncertainty in filter *l*, respectively, and N_{fit} is the total number of filters in the photometry, while *b* is the mean magnitude difference between observed fluxes and template fluxes. Details about the classification of stars could be found in our previous papers about star counts (Du et al. 2003, 2004a).

Thus, we can obtain the spectral types and luminosity classes for stars in the BATC survey. After knowing the stellar type, the photometric parallaxes can be derived by estimating absolute stellar magnitudes. We adopted the absolute magnitude versus stellar type relation for main-sequence stars from Lang (1992). A variety of errors affect the determination of stellar distances. The first source of errors could be from photometric uncertainty; the second from the misclassification that affects the derivation of absolute magnitude. In addition, there may be an error by the contamination of binary stars in our sample. We neglect the effect of binary contamination on distance derivation. For binaries with equal mass components, the distance will be

Table 2. Direction and relative information for the BATC Galactic structure fields

Observed field	R.A.	Decl.	epoch	l (deg)	b (deg)	$E(B - V)$	i (Comp)
T485	8:38:02.00	44:58:38.0	1950.	175.7	37.8	0.03	21.0
T518	9:54:05.60	-0:13:24.4	1950.	238.9	39.8	0.03	19.5
T288	8:42:30.50	34:31:54.0	1950.	189.0	37.5	0.02	20.0
T477	8:45:48.00	45:01:17.0	1950.	175.7	39.2	0.03	20.0
T328	9:10:57.30	56:25:49.0	1950.	160.3	41.9	0.03	19.5
T349	9:13:34.60	7:15:00.5	1950.	224.1	35.3	0.03	20.5
TA26	9:19:57.12	33:44:31.3	2000.	191.1	44.4	0.01	20.0
T291	9:32:00.30	50:06:42.0	1950.	167.8	46.4	0.01	20.0
T362	10:47:55.40	4:46:49.0	1950.	245.7	53.4	0.03	20.0
T330	11:58:02.90	46:35:29.0	1950.	147.2	68.3	0.00	20.5
U085	12:56:04.35	56:53:36.6	1996.	121.6	60.2	0.01	21.0
T521	21:39:19.48	0:11:54.5	1950.	56.1	-36.8	0.06	20.5
T491	22:14:36.10	-0:02:07.6	1950.	62.9	-44.0	0.03	20.0
T359	22:33:51.10	13:10:46.0	1950.	79.7	-37.8	0.06	20.5
T350	11:36:44.16	12:14:45.4	1950.	251.3	67.3	0.00	19.5
T534	15:14:34.80	56:30:33.0	1950.	91.6	51.1	0.01	21.0
T193	21:55:34.00	0:46:13.0	1950.	59.8	-39.7	0.05	20.0
T516	0:52:50.08	0:34:52.6	1950.	125.0	-62.0	0.00	20.0
T329	9:53:13.30	47:49:00.0	1950.	169.9	50.4	0.01	21.0
TA01	0:46:26.60	20:29:23.0	2000.	135.7	-62.1	0.00	20.5
T517	3:51:43.04	0:10:01.6	1950.	188.6	-38.2	0.12	20.0

NOTES.— Units of right ascension are hours, minutes, and seconds, and units of declination are degrees, arcminutes, and arcseconds.

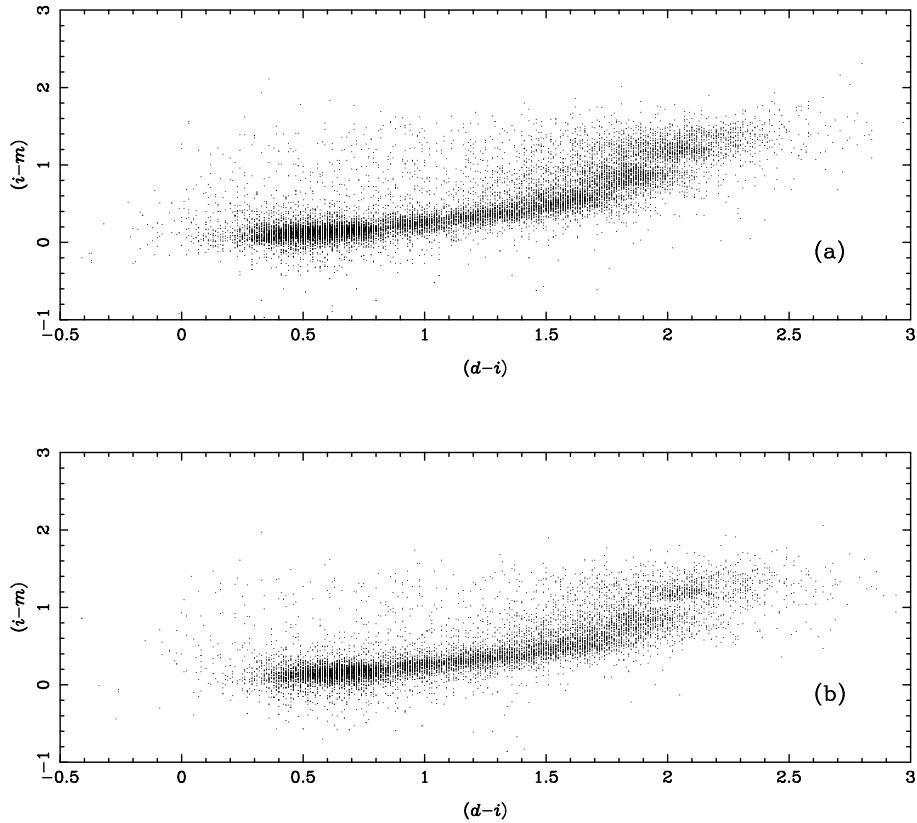


Figure 1. The distribution of $(i - m)$ versus $(d - i)$ for (a) the northern sample (north of the Galactic plane), (b) southern sample (south of the Galactic plane) down to the limiting magnitude.

Table 3. The colour-magnitude interval for the statistical discrimination of the three components

stellar populations i	thin disk	thick disk ($d - i$)	halo
(13.0-15.5]	≥ 0.9	< 0.9	-
(15.5-16.5]	≥ 0.9	< 0.9	-
(16.5-17.5]	≥ 1.0	< 1.0	-
(17.5-18.5]	≥ 0.9	[0.7-0.9)	< 0.7
(18.5-19.5]	≥ 0.9	-	< 0.9
(19.5-20.5]		≥ 1.2	< 1.2

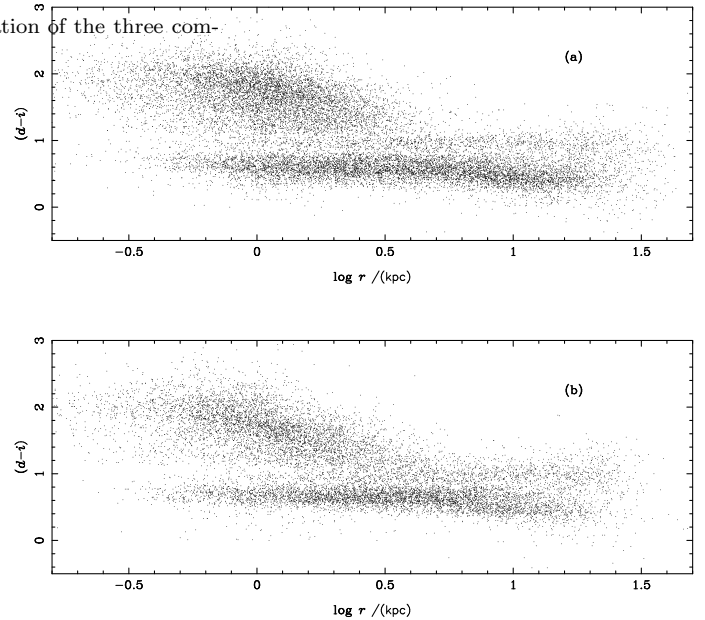
assumed closer by a factor of $\sqrt{2}$ (Ojha et al. 1996). Due to the unknown but probable mass distribution in binary components, the effect is certainly less severe (Majewski 1992; Kroupa et al. 1993). Since most fields are at intermediate and high latitude ($b > 35^\circ$), the error from the interstellar extinction in distance calculation can be neglected.

4 THE STELLAR DENSITY DISTRIBUTION

It is well known that the population types are a complex function of both colour and apparent magnitude. Standard star count models indicate that the colour-magnitude range could be used to separate roughly different populations of the Galaxy. In Fig. 2, the ($d - i$) colour distribution of the sample stars shows a bimodal distribution. The left-hand peak is dominated by halo stars, while the one on the right is dominated by thin disk stars, and the overlap between the halo stars and the thin disk stars is dominated by thick disk stars. Because halo stars are far more distant than the bulk of the disk stars, only the luminous stars in the halo (predominantly main-sequence stars) can be detected. For the main sequence stars, the intrinsically bright ones have bluer colour. Besides, the halo stars are generally more metal poor, and hence tend to dominate the blue peak. Similarly, the thin disk stars would form the red peak and the thick disk stars would lie between them. From this figure, we can see that the thick disk and halo populations overlap in the range ($d - i$) < 1.4 .

The colour distribution of the sample stars in the T288 field is given as a function of apparent magnitude in Fig. 3. According to Chen et al. (2001), the thick disk has a turnoff of $(g' - r')_0 = 0.33$ and it is dominant at bright apparent magnitudes, $15 < g'_0 < 18$ mag, whereas the halo has a turnoff colour at $(g' - r')_0 = 0.20$ for the apparent magnitude fainter than $g'_0 \sim 18$ mag. Karaali et al. (2003) also consider that the corresponding turnoff colour in the $UBVRI$ system are $(B - V)_0 = 0.41$ and 0.53 for halo and thick disk, respectively. In Fig. 4, we show the observed colour-magnitude diagram (i , $d - i$) from the the northern and the southern sample. Contrary to the distribution in Fig. 2, the thick disk and halo stars can be distinguished from the Fig. 3. For example, the apparent of a halo turnoff is apparent near $i = 17.5$, ($d - i$)=0.7. The turnoffs for the disk and halo in our sample are fixed (Table 3). Halo stars dominate the absolutely bright intervals, thick disk stars indicate the intermediate and the thin disk stars the faint ones.

Most of previous studies were based on the assumption of a suitable spatial density distribution, and on the

**Figure 5.** Spatial distribution of ($d - i$), and the photometric distances are derived according to the stellar type.

observational luminosity function and colour-magnitude diagram for each stellar population to fit the structural parameters and to interpret them by simulating the distribution of colour and magnitudes (Gilmore & Reid 1983). Here, on account of the use of the photometric parallaxes, we can make a direct evaluation of the spatial density law. Rather than trying to fit the structure of the Galaxy in the observed parameter space of colour and magnitudes, we transfer the observations into discrete density measurements at various points in the Galaxy.

In this study, the fields are located at intermediate and high latitudes, so neither a bulge component nor spiral arms are needed to describe the observation. The adopted model of stellar density distribution in this paper includes only two disks (thin disk and thick disk) and a halo. We try to derive the structural parameters (e.g. scale height) of the thin and thick disk populations using our data set. For this we calculate the stellar space density as a function of distance from the Galactic plane. At first, we use the two dimensional distribution of stars in the ($d - i$) vs. $\log r$ diagram (Fig. 5) to correct for this incompleteness. The nearest bins are assumed to be complete; for the incomplete bins we multiply iteratively by a factor given by the ratio of complete to incomplete number counts in the previous bin (Phleps et al. 2000). With the corrected number counts, the density in the log arithmetic space volume bins V_j can then be calculated according to

$$\rho_j = \frac{N_j^{corr}}{V_j} \quad (2)$$

here, $V_j = (\pi/180)^2(\omega/3)(r_{j+1}^3 - r_j^3)$ is partial volume, r_{j+1} and r_j are the limiting distances; and ω is field size in square degrees.

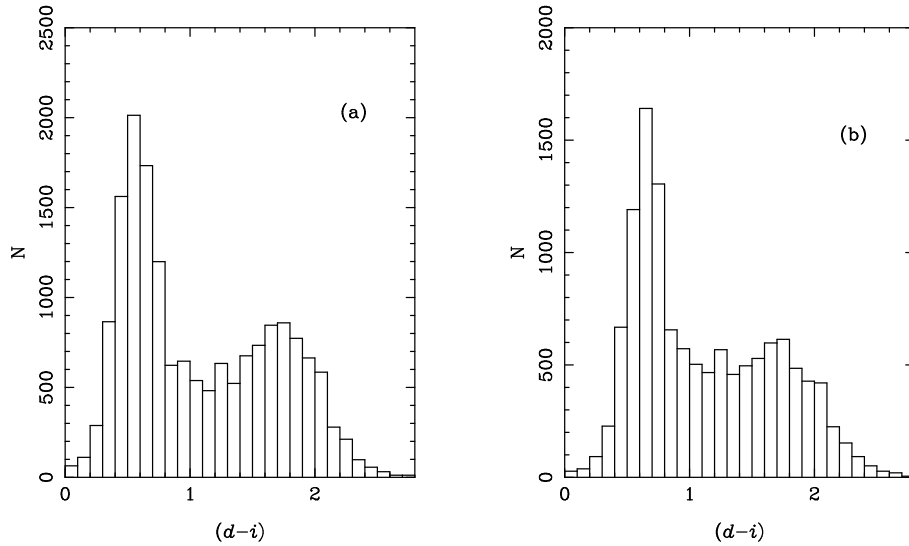


Figure 2. The $(d-i)$ colour distribution of the sample stars in the northern and the southern fields.

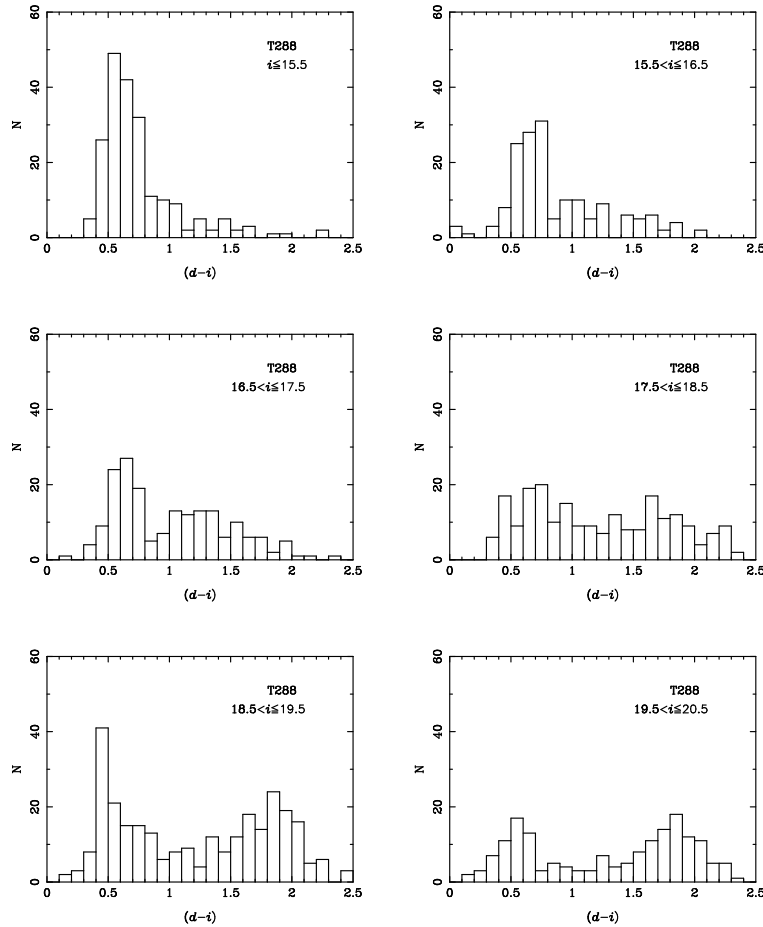


Figure 3. Colour distribution for the T288 field in our sample as a function of apparent magnitude.

4.1 Stellar density distribution in the disk

We have used a family of standard density laws to describe the populations of the Milky Way Galaxy. Disk structures are usually parameterized in cylindrical coordinates by radial and vertical exponential,

$$\rho(z, r) = \rho_0 e^{-z/h_z} e^{-(x-R_0)/h_l}, \quad (3)$$

where z is vertical distance from the Galactic plane, x is the Galactocentric distance in the plane, R_0 is the solar distance to the Galactic center (8.5 kpc), ρ_0 is the normalized local density, h_z and h_l are the scale height and scale length

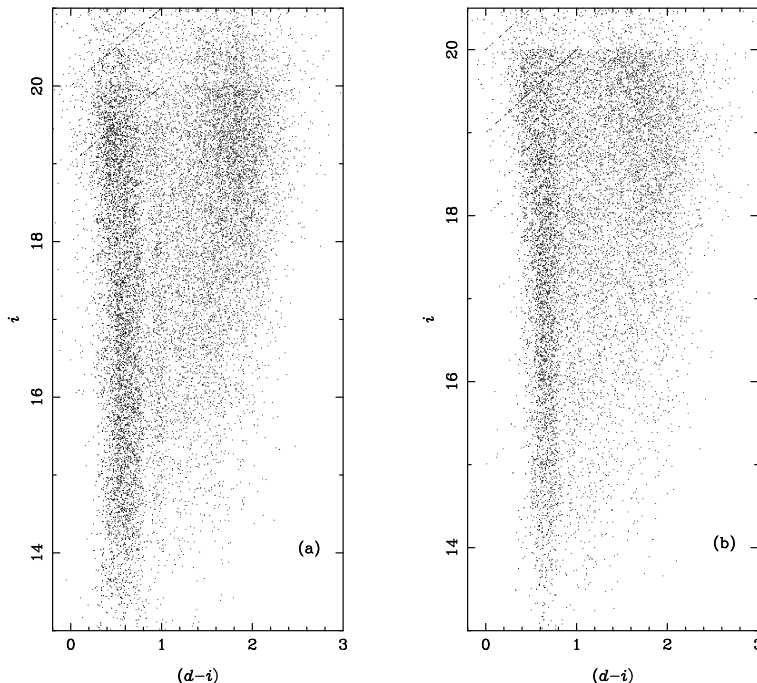


Figure 4. Observed $(i, d - i)$ colour-magnitude diagram from (a) the northern sample and (b) the southern sample

of disk, respectively. A similar form uses the sech^2 function to parameterize the vertical distribution:

$$\rho(z, r) = \rho_0 \text{sech}^2(-z/z_0) e^{-(z-R_0)/h_1}. \quad (4)$$

A squared secans hyperbolicus is the sum of two exponentials. The functional form represents a self-gravitating isothermal disk, and it avoids a singularity at $z = 0$. Some studies show the sech^2 fits better relative to the exponential density for faint absolute magnitude intervals for the thin disk in the optical star counts (Gould et al. 1996, Bilir et al. 2005). However, Hammersley et al. (1999) have shown that an exponential distribution, despite the singularity problems, is a much better fit to the infrared star counts of the Galaxy. In addition, Phleps (2000) have shown that there is a only minor difference between sech^2 hyperbolicus and exponential fit when the distance is less than 1 kpc. At large distances, the sech^2 function approximates the observed exponential density profile. We have chosen to use exponential functional form in this paper. As long as vertical direction is considered, the equation is as follows,

$$\rho(z) = n_1 e^{(-z/h_1)} + n_2 e^{(-z/h_2)}, \quad (5)$$

h_1 and h_2 are the scale heights of the thin disk and thick disk, respectively.

Fig. 6 shows the resulting density distribution of the disk stars in the four fields as an example. The solid line represents a fit with a superposition of two exponentials, and the dashed line is the fit for the thin disk component. The comparison between data and models is made using a χ^2 -fit. The most likely values for thin disk scale height h_1 , thick disk scale height h_2 and the corresponding space number density normalization n_2/n_1 are given in Table 4. Here, the thick disk density normalization is given in comparison to the density of the thin disk at the sun. The errors of scale heights and the corresponding space number density

normalization are estimated at a 68% confidential level. We find that the scale height is variable with the direction. The range of scale height for the thin disk vary from 220 to 320 pc. An old disk with an exponential scale height lower than the canonical value (325 pc) has been indicated by some authors such as Gilmore (1984); Bahcall & Soneira (1984); Reid & Majewski (1993). Although 220 pc seems an extreme value, it is close to the lower limit in the literature. The range of scale height for the thick disk is from 600 to 1100 pc, and the corresponding space number density normalization is 7.0–1.0% of the thin disk. At the same time, it shows that the thick disk dominates star counts at distances between 1.5 and 4 kpc over the galactic plane.

Some results for the thin disk scale height have been published in the literature. For example, some authors (Gilmore 1984; Bahcall & Soneira 1984; Yoshii et al. 1987; Reid & Majewski 1993) derived a scale height of 325 pc for old-disk stars; Chen (2001) derived the scale height of the thin disk to be 330 pc using two large star count samples. However, Kuijken & Gilmore (1989) derived a scale height of 249 pc for the old-disk stars. Haywood (1994) showed, from an analysis of numerous star counts towards the pole using his self-consistent evolutionary model, that the thin disk scale height does not exceed 250 pc. Ojha (1999) also found that the scale height of the thin disk is 240 pc based on an analysis of two star count samples. Siegle et al. (2002) gave apparent scale height $Z_{0,thin} = 280 - 350$ pc. Our result for the thin disk scale height is in a range of 220–320 pc. Karaali et al. (2004) showed that the scale height for thin disk decreases from absolutely bright to faint stars in a range 265–495 pc. They discussed the large range of Galactic structure parameters and claimed that Galactic model parameters are absolute magnitude dependent (Bilir et al. 2006). It is clear that our derived thin disk scale height is close to the value presented by Siegle et al. (2002) and

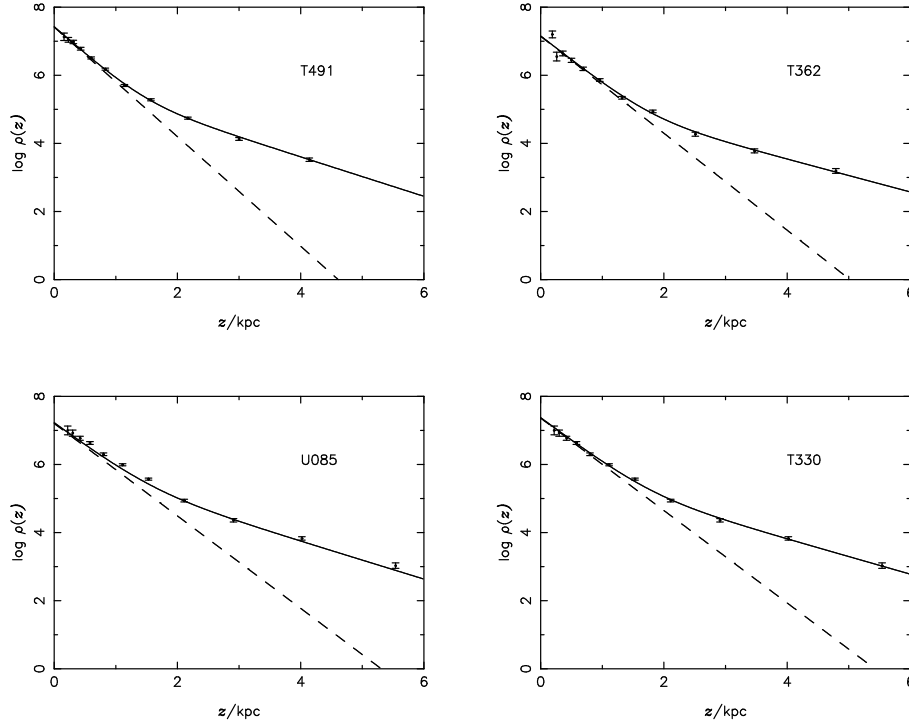


Figure 6. Vertical density distribution of the disk stars in the four field as a example. The solid line is a fit with a superposition of two exponentials, the dashed line is the single exponential fit for the thin disk component.

Karaali et al.(2004) from several selected areas. This is not a surprise, since most studies are based on investigation of one or a few fields in different directions.

The thick disk vertical structure is generally described as exponential with scale heights varying between 480 pc and 1500 pc and its local density is between 1% and 15% relative to the thin disk. Because of the small proportion of the thick disk locally with regard to the thin disk, it is difficult to derive a accurate scale height and local density of the thick disk. In general, any values of h_z in the range 480–1500 pc and of local density in 1%–15% turn out to be acceptable (Robin et al. 1996). The thick disk’s scale height is anticorrelated with its local density when fitted simultaneously in star count analysis, and a small scale height is obtained in combination with high local density, while large scale height is associated with low local density (Robin et al. 1996).

In some studies, the range of the parameters is large especially for the thick disk. For example, Gilmore (1984) presented a scale height of 1300 pc and local normalization of 2%, Kuijken & Gilmore (1989) derived a scale height of 1000 pc and local normalization of 4%. Robin et al. (1996) used broad-band multi-colour photometric and proper motion data to derive a scale height of $h_z = 760 \pm 50$ pc with a local density of $5.6 \pm 1.0\%$ relative to the thin disk. Spagna et al. (1996) used a *BVR* star count and proper motion data towards the NGP to derive the scale height of 1137 ± 61 pc with a local density of 4.3%. Ojha et al. (1999) presented a scale height of 790 pc with a local density of 6.1% of the thin disk from a photometry and proper-motion survey in the two directions at intermediate latitude. Chen (2001) gave a thick disk scale height between 580 pc and 750 pc, with a local density of 13–6.5% of the thin disk. Siegel et al.

(2002) also investigated these parameters, matching their Galactic model against deep multi-colour star count data for seven fields spinning a range of latitude and longitude. They derived a thick disk scale height of 740 pc with an 8.5% normalization to the old disk. Our derived results in this work show the thick disk scale height of 600–1100 pc, with a corresponding density normalization is 7.0–1.0% of the thin disk.

In summary, the scale height derived from various studies show large divergence, which cannot simply be attributed to statistical errors. There could be a number of reasons why the scale height varies with the observed direction in our study. The first reason could be from photometric parallaxes uncertainty arising from either misclassification or metallicity correction. But, unless the parallax correction is incorrect, this would not produce the effects we are seeing. The second possibility is that our adopted models assume the scale height is constant with radius from the Galactic center. However, maybe the disk (mainly the thick disk) is flared, with a scale height that increases with radius. This possibility is also mentioned in Siegel et al. (2002). In addition, it is clear that star counts when restricted to a small number of Galactic directions and a small magnitude range do not give a strong constraint on the scale height.

4.2 Stellar density distribution in the halo

Among all of the Galaxy’s populations, the halo is traditionally expected to have changed the least since it formed, and therefore it provides important clues to the Galaxy’s formation and evolution. The halo is not only less massive than the disk, but also it occupies a much larger volume than the disk (Larsen & Humphreys 2003). According to the study-

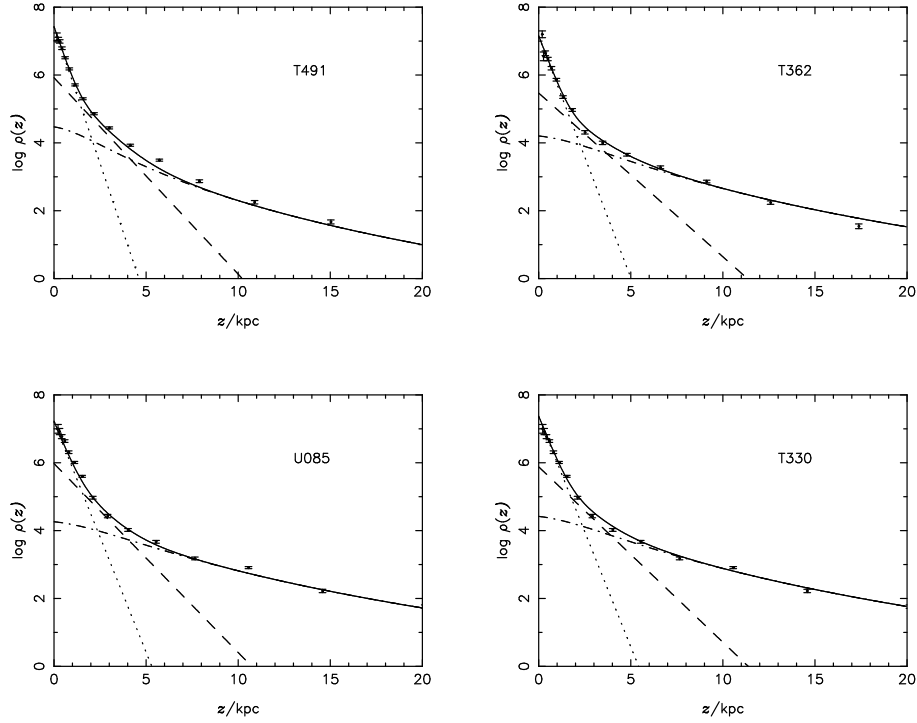


Figure 7. Density distribution perpendicular to the Galactic plane, the dotted line shows the contribution of the thin disk component, the dashed line is the contribution of the thick disk, the dot-dashed line is a de Vaucouleurs law and the solid line the sum of the three.

Table 4. The Galactic structure parameters derived from fields in this study.

field name	thin disk h_1 (pc)	thick disk h_2 (pc)	thick disk local normalization	halo axis ratio
T485	310 ± 17	930 ± 20	0.010	0.70
T518	220 ± 17	600 ± 15	0.026	0.37
T288	265 ± 20	810 ± 25	0.021	0.67
T477	280 ± 25	1020 ± 25	0.010	0.67
T328	245 ± 25	720 ± 15	0.030	0.46
T349	260 ± 16	600 ± 30	0.026	0.49
TA26	230 ± 17	690 ± 30	0.021	0.50
T291	290 ± 23	810 ± 25	0.019	0.58
T362	305 ± 30	900 ± 30	0.021	0.61
T330	320 ± 12	840 ± 30	0.033	0.58
U085	320 ± 15	780 ± 23	0.059	0.64
T521	305 ± 20	810 ± 20	0.012	0.43
T491	270 ± 20	750 ± 30	0.032	0.40
T359	255 ± 30	600 ± 20	0.039	0.40
T350	310 ± 19	1050 ± 30	0.024	0.64
T534	300 ± 20	720 ± 20	0.048	0.58
T193	250 ± 30	600 ± 20	0.069	0.40
T516	240 ± 20	750 ± 25	0.028	0.50
T329	320 ± 15	640 ± 30	0.068	0.60
TA01	320 ± 20	960 ± 15	0.019	0.61
T517	220 ± 10	750 ± 30	0.010	0.44

ing for the photographic plates of nearby galaxies, there are numerous forms for the density law of spheroid components. The de Vaucouleurs law is most used to describe the surface brightness profile of elliptical galaxies. The de Vaucouleurs law is an empirical description of the density distribution of the Galactic halo. The analytic approximation is:

$$\rho_s(R, b, l) = \rho_0 \frac{\exp[-10.093(\frac{R}{R_\odot})^{1/4} + 10.093]}{(\frac{R}{R_\odot})^{(7/8)}} \times 1.25 \frac{\exp[-10.093(\frac{R}{R_\odot})^{1/4} + 10.093]}{(\frac{R}{R_\odot})^{(6/8)}}, \quad R < 0.03R_\odot$$

$$\times [1 - 0.08669/(R/R_{\odot})^{1/4}], \quad R \geq 0.03R_{\odot}$$

where $R = (x^2 + z^2/\kappa^2)^{1/2}$ is Galactocentric distance, κ is the axis ratio, $x = (R_{\odot}^2 + d^2\cos^2b - 2R_{\odot}d \cos b \cos l)^{1/2}$, $z = d \sin b$; $R_{\odot} = 8$ kpc is the distance of the sun from the Galactic center, b and l are the Galactic latitude and longitude; the normalization factor ρ_0 is usually expressed as a percentage of the local spatial density of stars.

Other models have used the power-law form,

$$\rho_s(R) = \rho_0/(a_0^n + R^n), \quad (7)$$

where a_0 is the core radius (an often omitted parameter).

Although Ng et al. (1997) claimed that a halo population described as a $r^{1/4}$ law predicts less stars than power law at fainter magnitudes, the choice of halo density is somewhat arbitrary since the difference between de Vaucouleurs law and power law are subtle when seen through such a roughly ground lens as star counts. In our analysis, we use the blue stars (Table 3) to distinguish the population of halo stars from our sample stars. We adopted a de Vaucouleurs law for the halo component of the Galaxy and local density normalization $\rho_0 = 0.125\%$ in the model. Fig. 7 gives the density distribution of all stars in the four fields as an example. The dotted line shows the contribution of the thin disk component; the dashed line is the contribution of the thick disk; the dot-dashed line is a de Vaucouleurs law, and the solid line is the sum of the three components. It can also be seen that the corresponding plots fit the distribution of the halo stars up to distance of over 15 kpc above the Galactic plane. Our counts imply that the axis ratio of the stellar halo varies from 0.4 to 0.7.

From our sample fields, T521, T491, T359, T193 and T534 should belong to the inner part of the halo, while the others lie in the outer part of the halo according to their longitude and latitude. The axis ratio versus the longitude distribution is shown in Fig. 8. It is clear that the axis ratio towards the Galactic center is somewhat flatter (~ 0.4), while the shape of the halo in the anticentre and antirotation direction is rounder with $c/a > 0.4$. For T518, the deviant result may reflect a fluctuation in the Galactic density distribution, or a systematic error in the observational data. In summary, star counts in different lines of sight can be used directly to obtain a rough estimate of the shape of the stellar halo, although a dependency on models enters through isolating halo stars. Besides, since our sample fields are not in the lower latitude areas, which were noted to have asymmetry (Larsen & Humphreys 1996; Newberg & Yanny 2005; Xu et al. 2006), we cannot detect the triaxial halo distribution.

The apparent discrepancy of the halo axis ratio from various studies may be due to the multi-component nature of the Galactic halo (Buser & Kaeser 1985). Hartwick (1987) found that the metal-poor globular clusters and RR Lyrae stars both had a spatial distribution that was better fitted by two components; the inner component, which dominates in the solar neighborhood, is flattened with an axis ratio of ~ 0.6 , while the outer component is spherical. Kinman et al. (1994) also found evidence for two components, one significantly flattened which dominates locally, and one more spherical, in their sample of halo blue horizontal branch stars. Some studies of the kinematics and abundance of both field stars and globular clusters show that the halo is better

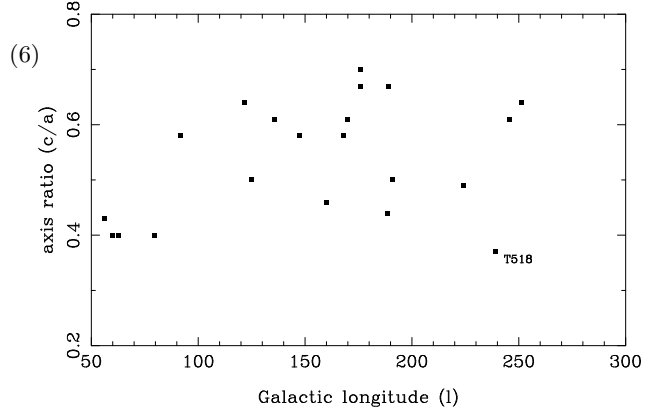


Figure 8. The halo axis ratio distribution versus the the Galactic longitude

described as having two sub-populations—a flattened inner halo and a spherical outer halo (Siegel et al. 2002). Additional support for dual-halo models can be drawn from the apparent dichotomy in detailed chemical abundance of halo stars (Nissen & Schuster 1997). In a dual-halo model, nearby stars (Larsen & Humphreys 1994, 2003; Wyse & Gilmore 1989; Lemon et al., 2004; Siegel et al. 2002; this work) are dominated by the flattened inner halo while distant stars are dominated by the round outer halo (Koo et al. 1986; Bahcall & Soneira 1984; Preston et al. 1991).

The principal contribution of star counts in constraining Galactic formation scenarios lies in revealing the underlying shape, chemistry and ages of the stellar population through sophisticated modelling. Our study of stellar halo provides some support for the hybrid formation model. The existence of two components may be evidence that the stellar halo formed by hybrid collapse process (Wyse 1995; Van den Bergh 1993; Zinn 1993; Norris et al. 1994; Chiba & Beers 2000), or that the stellar halo is locally flattened in response to the disk potential (Binney & May 1986), or perhaps reflects the different orbital parameters and internal structure of disrupted satellite galaxies that were accreted by the Galaxy to form the stellar halo (Freeman 1987).

5 SUMMARY AND DISCUSSION

We have analyzed the BATC survey data observed in 21 fields with the help of a Galaxy model in order to parameterize the vertical distribution of stars in the Milky Way. The adopted model of the Galaxy consists of three components: thin disk, thick disk (exponential form) and halo (de Vaucouleurs law). From the χ^2 fit to the direct measurement of the stellar density distribution, we determine that the range of scale height for the thin disk varies from 220 to 320 pc. Although 220 pc seems an extreme value, it is close to the lower limit in the literatures. The range of scale height for the thick disk is from 600 to 1100 pc, and the corresponding space number density normalization is 7.0–1.0% of the thin disk. Our results show that the scale height is variable with the observation direction, which cannot be attributed to statistical errors. Possibly the main reasons can be attributed to the disk (mainly the thick disk) is flared, with a scale height that increases with radius. It is consistent with merger origin

for the thick disk formation. The actual numerical values of Galactic structure parameters are less scientifically important than what they tell us about the Galaxy in general – for example, the origin of the populations. A number of scenarios have been proposed for the origin of the thick disk (see review in Majewski 1993 and Siegel et al. 2002).

In addition, adopting a de Vaucouleurs $r^{1/4}$ law halo and a local density normalization $\rho_0 = 0.125\%$, we find that the axis ratio towards the Galactic center is more flatter (~ 0.4), while the shape of the halo in the anticentre and antirotation direction is rounder with $c/a > 0.4$. It reflects the shape of the inner halo. In a word, the star counts in different lines of sight can be used directly to obtain a rough estimate of the shape of the stellar halo. With completeness limits for our selected fields typically 19th to 21th magnitude, our star counts are most applicable to the inner halo. Our solutions support the Galactic models with a flattened inner halo. The inner halo is difficult to distinguish from the thick disk, and it is chemically and kinematically overlapped the thick disk – possibly formed by a merger early in the Galaxy's history. The outer halo is more or less spherical and is disjoint from the inner halo. In particular, the outer halo might be dominated by substructures that are likely the remnants of interactions.

Evidence has been growing for some time that simple description of the Galactic halo are inadequate. It is possible that the axis ratio may vary with distance, and the halo becomes more spherical in the outer parts. Some surveys have also found a single axis ratio too restrictive and adopted a axis ratio (c/a) that increases with Galactocentric radius to explain the stellar spatial distribution in the halo. The dual halo models may resolve many of the disagreements in star count results. However, answering the question of whether or not the multi-component or triaxial halo is supported requires more data such as kinematics and chemical abundances analysis. The question will be resolved with the coming on-line of future projects aimed at spectroscopic sky surveys such as SEGUE, LAMOST, GAIA, and further photometric surveys of the southern sky.

ACKNOWLEDGMENTS

The BATC Survey is supported by the Chinese Academy of Sciences, the Chinese National Natural Science Foundation under the contract No. 10473012 and No. 10573020, the Chinese State Committee of Sciences and Technology. This work was also supported by the GUCAS president fund yzjj200501.

REFERENCES

- Bahcall, J. N., Soneira, R. M., 1980, *ApJs*, 44, 73
 Bahcall, J. N., Soneira, R. M., 1984, *ApJs*, 55, 67
 Bilir, S., Karaali, S., Tuncel, S., 2005, *AN*, 326, 321
 Bilir, S., Karaali, S., Gilmore, G., 2006, *MNRAS*, 366, 1295
 Binney, J., May, A., 1986, *MNRAS*, 218, 743
 Brook, C. B., Gibson, B. K., Martel, H., et al., 2005, *ApJ*, 630, 298
 Burstein, D., Heiles, C., 1982, *AJ*, 87, 1165
 Buser, R., Kaeser, U., 1985, *A&A*, 145, 1
 Buser, R., Rong, J., Karaali S., 1999, *A&A*, 348, 98
 Chen, B., Stoughton, C., Smith, A., 2001, *ApJ*, 553, 184
 Chiba, M., Beers, T. C., 2000, *AJ*, 119, 2843
 Du, C. H., Zhou, X., Ma, J., et al., 2003, *A&A*, 407, 541
 Du, C. H., Zhou, X., Ma, J., Chen, J.S., 2004, *Chin. Phys. Lett.*, 6, 1179
 Du, C. H., Zhou, X., Ma J., Shi, Y.R., et al., 2004, *AJ*, 128, 2265
 Fan, X. H., et al. 1996, *AJ*, 112, 628
 Freeman, K. C., 1987, *ARA&A*, 25, 603
 Fukugita, M., Ichikawa, T., Gunn, J. E., et al. 1996, *AJ*, 111, 1748
 Gilmore, G., Reid, N., 1983, *MNRAS*, 202, 1025
 Gilmore, G., 1984, *MNRAS*, 207, 223
 Gilmore, G., Wyse, R. F. G., 1985, *AJ*, 90, 2015
 Gilmore, G., Wyse, R. F. G., Kuijken, K., 1989, *ARA&A*, 27, 555
 Gould, A., Bahcall, J.N., Flynn, C., 1996, *ApJ*, 465, 759
 Hartwick, F. D. A., 1987, in the *Galaxy*, ed. G. Gilmore and R. Carswell (Dordrecht, Reidel), p. 413
 Hammersley, P. L., Cohen, M., Garzn, F., et al., 1999, *MNRAS*, 308, 333
 Haywood, M., 1994, *A&A*, 282, 444
 Jenkner, H., Lasker, B. M., Sturch, C. R., et al. 1990, *AJ*, 99, 2082
 Kaempf, T. A., de Boer, K. S., Altmann, M., 2005, *A&A*, 432, 879
 Karaali S., AK, S. G., Bilir, S., Karatas, Y., Gilmore, G., 2003, *MNRAS*, 343, 1013
 Karaali, S., Bilir, S., Hamzaoglu, E. 2004, *MNRAS*, 355, 307
 Kinman, T. D., Suntzeff, N. B., Kraft, R. P., 1994, *AJ*, 108, 1722
 Koo, D. C., Kron, R. G., Cudworth, K. M., 1986, *PASP*, 98, 285
 Kroupa, P., Tout C. A., Gilmore, G., 1993, *MNRAS*, 262, 545
 Kuijken, K., Gilmore, G., 1989, *MNRAS*, 239, 605
 Lang, K. R., 1992, *Astrophysical Data I, Planets and stars*, Berlin, Springer-Verlag
 Larsen, J. A., Humphrey, R.M., 1994, *ApJ*, 436, 149
 Larsen, J. A., Humphrey, R.M., 1996, *ApJ*, 468, 99
 Larsen, J. A., Humphreys, R. M., 2003, *AJ*, 125, 1958
 Lemon, D. J., Wyse, R. F. G., Liske, J., Driver, S. P., et al., 2004, *MNRAS*, 347, 1043
 Majewski, S. R., 1992, *ApJs*, 78, 87
 Majewski, S. R., 1993, *ARA&A*, 31, 575
 Méndez, R. A., Minniti, D., de, M. G., et al., 1996, *MNRAS*, 283, 666
 Newberg, H. J., Yanny, B., preprint (astro-ph/0507671)
 Nissen, P. E., Schuster, W. J., 1997, *A&A*, 326, 751
 Ng, Y. K., Bertelli, G., Chiosi, C., Bressan, A., 1997, *A&A*, 324, 65
 Norris, J. P., 1994, *ApJ*, 431, 645
 Oke, J. B., Gunn, J. E., 1983, *ApJ*, 266, 713
 Ojha, D. K., Bienayme, O., Robin, A. C., et al. 1996, *A&A*, 311, 456
 Ojha, D. K., Bienayme, O., Mohan, V., Robin, A.C., 1999, *A&A*, 351, 945
 Peiris, H. V., 2000, *ApJ*, 544, 811
 Pohlen, M., Balcells, M., Ltticke, R., Dettmar, R. J., 2004, *A&A*, 422, 465

- Phleps, S., Meisenheimer, K., Fuchs, B., Wolf, C., 2000, A&A, 356, 108
- Pickles, A. J., 1998, PASP, 110, 863
- Preston, G. W., Shectman, S. A., Beers, T. C., 1991, ApJ, 375, 121P
- Reid, I. N., Majewski, S. R., 1993, ApJ, 409, 635
- Reid, I. N., Yan, L., Majewski, S., et al., 1996, AJ, 112, 1472
- Robin, A. C., Cr ez e, M., 1986, A&A, 157, 71
- Robin, A. C., Haywood, M., Cr ez e, M., 1996, A&A, 305, 125
- Robin, A. C., Reyl e, C., Derri ere S., et al., 2003, A&A, 409, 523
- Siegel, M. H., Majewski, S. R., Reid, I. N., 2002, ApJ, 578, 151
- Spagna, A., Lattanzi, M. G., Lasker, B. M., 1996, A&A, 311, 758
- Stetson, P. B., 1987, PASP, 99, 191
- Van den Bergh, S., 1993, ApJ, 411, 178
- Wyse, R. F. G., Gilmore, G., 1986, AJ, 91, 855
- Wyse, R. F. G., Gilmore, G., 1989, MNRAS, 239, 605
- Wyse, R. F. G., 1995, PASP, 107, 785
- Xu, Y., Deng, L.C., Hu, J.Y., 2006, preprint (astro-ph/0602565)
- Zhou, X., Jiang, Z. J., Xue, S. J., Wu, H., Ma, J., Chen, J. S. 2001, ChJAA, 1, 372
- Zhou, X., et al. 2003, A&A, 397, 361
- Zinn, R., 1993, in The Globular Cluster-Galaxy Connection, ed. G.H. Smith and J.P. Brodie (San Francisco, ASP), p. 38